A one-dimensional chain state of vortex matter

Alexander Grigorenko*, Simon Bending*, Tsuyoshi Tamegai†, Shuuichi Ooi† & Mohamed Henini‡

** Department of Physics, University of Bath, Claverton Down, Bath, BA2 7AY, UK*
† Department of Applied Physics, University of Tokyo, Hongo, Bunkyo-ku, Tokyo 113-8627, Japan, and CREST, Japan Science and Technology Corporation (JST), Japan
‡ Department of Physics, University of Nottingham, Nottingham, NG7 2RD, UK

Magnetic flux penetrates isotropic type II superconductors in flux-quantized vortices, which arrange themselves into a lattice structure that is independent of the direction of the applied field[1]. In extremely anisotropic high-transition-temperature (high-T_c) superconductors, a lattice of stacks of circular 'pancake' vortices forms when a magnetic field is applied perpendicular to the copper oxide layers, while an orthogonal elongated lattice of elliptical Josephson vortices forms when the applied field is parallel to the layers[2–5]. Here we report that when a tilted magnetic field is applied to single crystals of $Bi_2Sr_2CaCu_2O_{8+\delta}$, these lattices can interact to form a new state of vortex matter in which all stacks of pancake vortices intersect the Josephson vortices. The sublattice of Josephson vortices can therefore be used to manipulate the sublattice of pancake vortices. This result explains the suppression of irreversible magnetization by in-plane fields as seen in $Bi_2Sr_2CaCu_2O_{8+\delta}$ crystals, a hitherto mysterious observation[6]. The ability to manipulate sublattices could be important for flux-logic devices, where a 'bit' might be represented by a pancake vortex stack, and the problem of vortex positioning is overcome through sublattice interactions. This also enables the development of flux transducers and amplifiers, considerably broadening the scope for applications of anisotropic high-T_c superconductors.

The structure and organization of superconducting vortices directly reflects the crystalline anisotropy of the host material (Fig. 1A–D). A consequence of the extremely high anisotropy exhibited by $Bi_2Sr_2CaCu_2O_{8+\delta}$ (BSCCO) single crystals is that tilted vortices spontaneously decompose into interacting 'crossing lattices' of pancake vortex (PV) and Josephson vortex (JV) stacks[3–5] (Fig. 1E) whose phases remain largely unexplored. We show here the formation of a one-dimensional (1D) chain state of vortex matter in this regime, when all pancake vortex stacks become trapped on underlying stacks of Josephson vortices (Fig. 1F). This phase is bounded by transitions to a composite lattice[7,8] of chains in a hexagonal lattice matrix at low tilt angles, and by a 'sublimed' chain state at high tilt angles.

We have used high-resolution scanning Hall probe microscopy[9] to explore the crossing-lattices phase diagram in BSCCO single crystals under independently applied c-axis (H_c) and in-plane ($H_{//}$) magnetic fields. Magnetic images are generated parallel to the crystallographic a–b surface of freshly cleaved crystals with a lateral resolution of a few hundred nanometres, and the Hall probe typically detects the top 300 pancake vortices in a stack whose flux threads it along the c axis. The location of stacks of JVs is inferred from the fact that they become 'decorated' by PVs owing to their mutual attraction, in analogy with the well known Bitter decoration technique with fine ferromagnetic particles.

Figure 2A shows a typical set of images, obtained from scanning Hall probe microscopy, of the magnetic induction just above the face of a BSCCO single crystal as the angle between the applied field and the c axis was progressively increased. With a 12-Oe field parallel to the c axis at 81 K (Fig. 2A, a), a well-ordered hexagonal lattice of PV stacks was observed. However, as the in-plane field component ($H_{//}$) was increased from zero, 'chains' of PV stacks formed, which separated domains of approximately hexagonal PV lattice (Fig. 2A, b and c). As seen in earlier Bitter decoration experiments[7,8], the chains were aligned along the direction of the in-plane field, and the vortex separation within the chains was smaller than that of the Abrikosov lattice. As H_c is decreased below the 'ordering' field, when intervortex interactions become comparable to pinning forces[10], quenched disorder in the BSCCO crystal destroys the six-fold symmetry of the Abrikosov domains (Fig. 2A, d). As H_c is decreased still further, we observe a phase transition to another ordered 1D vortex chain state when the domains of Abrikosov lattice vanish entirely (Fig. 2A, e and f).

The crossing-lattices picture[3–5] explains the complex behaviour illustrated in Fig. 2, where chain formation arises owing to the

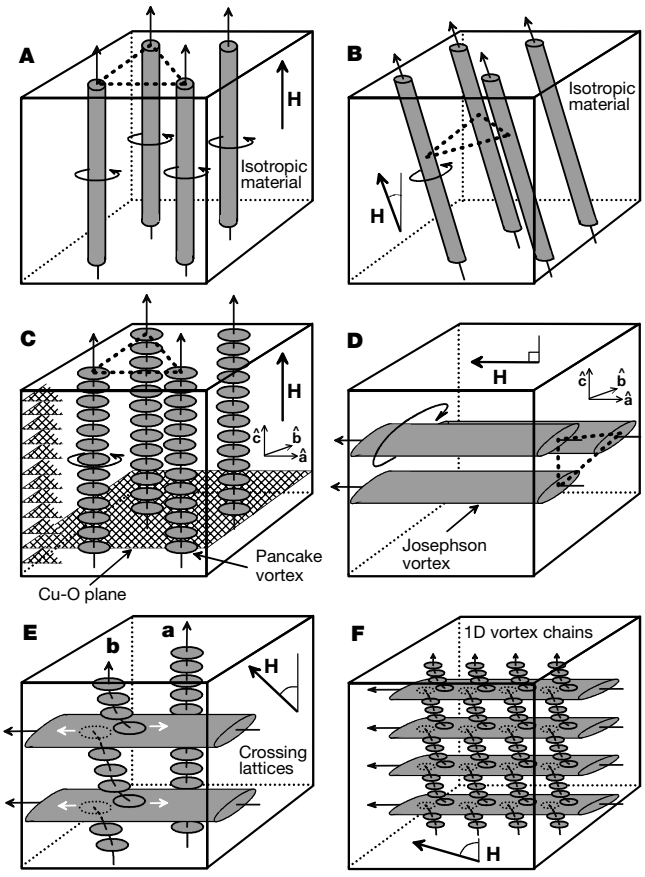

Figure 1 Sketches of vortex structures in isotropic and layered superconductors. **A**, **B**, The situation in an isotropic superconductor where the repulsion between vortices leads to the formation of an ordered hexagonal lattice independent of the tilt angle. Curved arrows indicate circulating supercurrents around the normal vortex core. **C**, Hexagonal ordering of the vortex lattice in layered superconductors with the magnetic field applied along the high-symmetry c axis. In this case, vortices are formed of vertical stacks of 2D pancake vortices situated in the Cu–O planes where superconductivity resides. **D**, With the magnetic field parallel to the layers, crystalline anisotropy leads to the formation of elliptical Josephson vortices whose 'cores' reside in the spaces between Cu–O planes, and whose circulating currents derive partly from strong supercurrents within the Cu–O planes and partly from weak Josephson coupling between them. Josephson vortices order into a highly elongated rhombic lattice. **E**, For a broad range of intermediate angles, tilted vortices spontaneously decompose into coexisting orthogonal PV and JV 'crossing lattices'. **a**, If stacks of PVs and JVs do not intersect, no direct interaction occurs. **b**, Where a PV stack intersects a JV stack, small PV displacements (indicated by white arrows) driven by the underlying JV supercurrents lead to an attractive interaction. **F**, Zoomed-out view of the 1D vortex chain state when all PV stacks become trapped on vertical stacks of JVs.

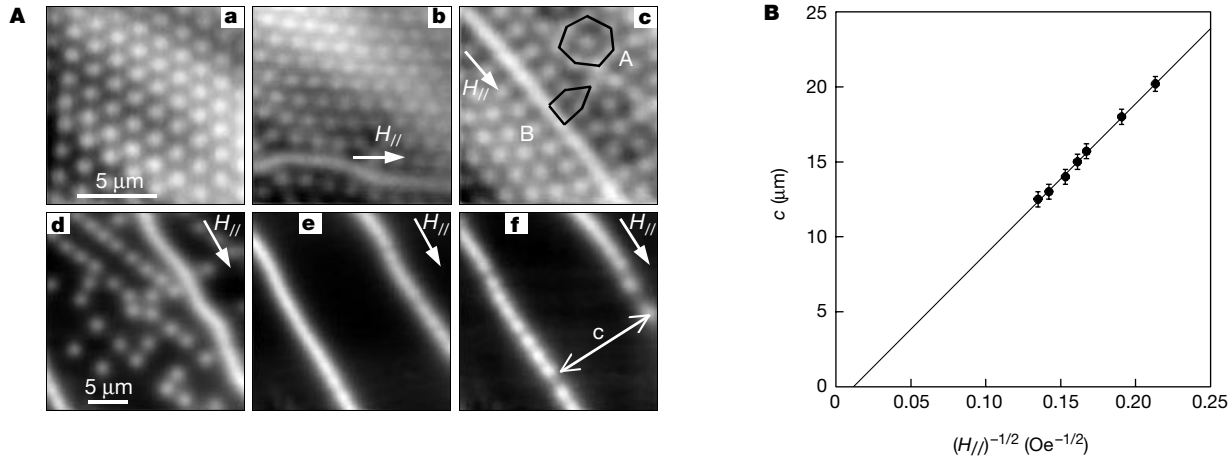

Figure 2 Images of stacks of pancake vortices in a BSCCO single crystal. The depth to which the Hall sensor probes the PV stacks in the as-grown crystals ($T_c = 90$ K) is roughly the in-plane magnetic penetration depth (typically the top 300 PVs in a stack). **A, a**, The hexagonal Abrikosov lattice of PV stacks obtained at $H_c = 12$ Oe ($H_{//} = 0$) at 81 K. (Greyscale spans 2.5 G.) The composite vortex lattice state is shown in **b** for $H_c = 14$ Oe and $H_{//} = 32$ Oe at 81 K (greyscale, 1.7 G), and for a different orientation of in-plane field (greyscale, 1.9 G) in **c** for $H_c = 10$ Oe and $H_{//} = 32$ Oe at 77 K. Arrows indicate the direction of the in-plane field. The presence of the incommensurate chains frustrates the surrounding hexagonal vortex lattice domains, giving rise, for example, to the seven-fold and five-fold rings indicated by A and B, respectively. **d**, The composite lattice state below the 'ordering' field at $H_c = 2$ Oe and $H_{//} = 27$ Oe at 81 K (greyscale, 2.9 G). The 1D vortex chain state is shown at **e**, $H_c = 1.2$ Oe and $H_{//} = 40$ Oe at 81 K (greyscale, 2.5 G), and with a lower density of PVs at **f**, $H_c = 0.5$ Oe and $H_{//} = 35$ Oe at 81 K. The chains of PV stacks in **e** and **f** are up to 50 in-plane penetration depths apart, and truly non-interacting. Comparing the PV–JV attraction and intra-chain PV–PV repulsion for the limit of non-overlapping JV cores[5], we find that the isolated chain state is stable when $H_c^2/H_{//} > \Phi_0/(\sqrt{3}\gamma\lambda_{ab}^2 \ln^2(c/c_0))$ where λ_{ab} is the in-plane penetration depth, $c_0 = A\lambda_{ab}^2/(\gamma s)$, A is a constant of order unity and s is the Cu–O plane separation. Experimentally we find that this ratio depends only weakly upon $H_{//}$, and is about 0.04 Oe at 77 K for our as-grown sample. **B**, Plot illustrating the linear dependence of the chain separation, c (as indicated in **A**, **f**), on $(H_{//})^{-1/2}$ at 81 K.

attraction of PVs to underlying stacks of JVs in the rhombic JV lattice, with an expected lateral separation of $c = [\sqrt{3}\gamma\Phi_0/(2H_{//})]^{1/2}$ (where γ is the anisotropy parameter and Φ_0 is the superconducting flux quantum). The measured chain separation, c, at 81 K is plotted as a function of $(H_{//})^{-1/2}$ in Fig. 2B, and the linear dependence allows us to evaluate directly the anisotropy parameter $\gamma = 580 \pm 20$, in reasonable agreement with other estimates[11]. PV stacks can always lower their energy by moving onto JV stacks provided that repulsive interactions with nearby pancake vortices do not become prohibitively large. Consequently the formation of

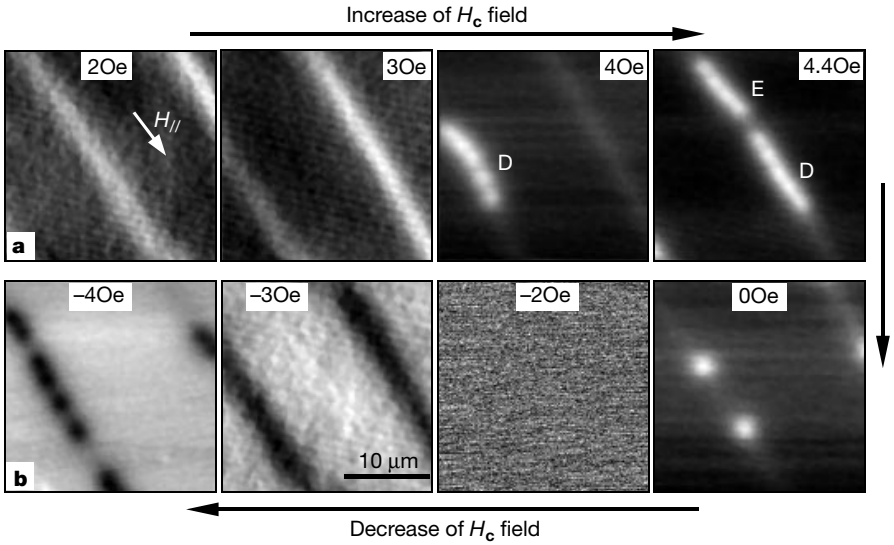

Figure 3 Images of pancake vortices in a BSCCO single crystal. This series of movie images shows the 'crystallization' and subsequent 'sublimation' of pancake vortex stacks after zero-field cooling to 83 K as the c-axis magnetic field is varied frame by frame, keeping the in-plane field fixed at $H_{//} = 38$ Oe. Each image takes ~12 s to acquire. (Entire movies and additional data are available at http://www.bath.ac.uk/~pyssb/.) **a**, H_c increasing. The 'sublimed' state is shown at $H_c = 2$ Oe (greyscale, 0.35 G) and 3 Oe (greyscale, 0.4 G), as well as the partially 'crystallized' state at $H_c = 4$ Oe (greyscale, 2.3 G) and 4.4 Oe (greyscale, 2.3 G). The coexistence of adjacent low flux density and high flux density regions seems to indicate that some form of phase separation has taken place. **b**, H_c decreasing. Shown are 'resublimation' of the crystallites as the field was reduced to $H_c = 0.0$ Oe (greyscale, 1.7 G), and the total expulsion of PVs at $H_c = -2.0$ Oe (greyscale, 0.14 G), as well as the sublimed state in the reverse direction at $H_c = -3$ Oe (greyscale, 0.3 G) and its 'crystallization' at $H_c = -4$ Oe (greyscale, 2.1 G). Note that the reversal of sign of the 'sublimed' stripes as H_c is reversed at fixed in-plane field indicates that we are detecting pancake vortices and not some component of the field from the Josephson vortices. We speculate that the 'sublimed' state is one where pancake vortex stacks decompose into tilted vortices composed of a staircase of individual pancakes, or short PV segments, linked by sections of JV. We expect these objects to exhibit very large thermal fluctuations at the high temperatures used in these experiments.

the 1D chain state (Fig. 1F) may be anticipated for small values of H_c when the spacing between PV stacks along the chain can be arbitrarily large.

The 1D vortex chain state is bounded by a transition to a composite lattice composed of chains embedded in a hexagonal lattice 'matrix' at low tilt angles (Fig. 2A, b and c). But at high tilt angles, the phase again becomes unstable, and a transition to a state composed of 1D chains of 'sublimed' PV stacks is observed. Figure 3 shows a series of images from a movie of the sublimation process as the phase boundary is crossed in both directions at 83 K by cycling H_c slowly at fixed $H_{//} = 38$ Oe. At very small c-axis fields, the 1D vortex chain is only visible as a structureless 'sublimed' stripe of very low flux density ($H_c = 2$ Oe and 3 Oe). The magnetic induction (hence the PV density) associated with the 'sublimed' stripe grows with increasing H_c, implying that PVs preferentially penetrate and travel along JV stacks. But as H_c is increased further, 'crystallites' of well resolved PV stacks, with ten times higher flux density, nucleate and grow ($H_c = 4$ Oe and 4.4 Oe). If H_c is reduced again, these crystallites 'resublime' ($H_c = 0$ Oe), and eventually all PVs leave the sample ($H_c = -2$ Oe). If the field is decreased further, the sublimed stripes reverse sign ($H_c = -3$ Oe), and the nucleation of 'black' crystallites occurs ($H_c = -4$ Oe). Sublimation processes of this type have not (to our knowledge) been previously considered, although the first-order melting of vortex crystals in BSCCO as the magnetic field is increased has been widely studied[12,13]. A second re-entrant melting phenomenon has also been theoretically predicted as the field is reduced in the solid phase; this transition is driven, not by an increase in entropy as for first-order melting, but by the exponential 'softening' of the crystal shear modulus at very low fields[14]. In contrast, we speculate that the transition to the 'sublimed' state corresponds to the shearing of PV stacks into tilted vortices composed of a staircase of isolated pancakes, or small pancake segments, linked by sections of Josephson vortex. Our experimentally established boundaries for the 1D vortex chain state are summarized in the experimental phase diagram for BSCCO single crystals under tilted magnetic fields shown in Fig. 4.

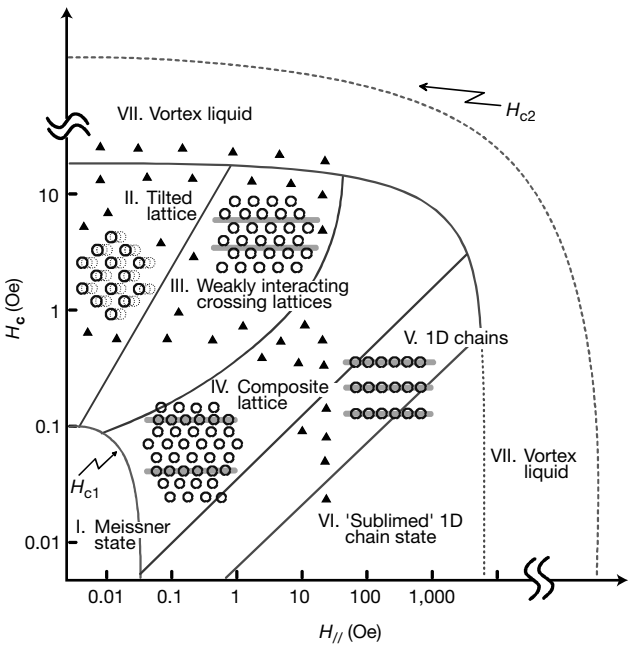

Figure 4 Experimental phase diagram for vortex matter in BSCCO single crystals. Our experimental data (filled triangles) have been used to map out a phase diagram for the different observed states of vortex matter in the H_c–$H_{//}$ domain for the temperature range where this study was performed (77–88 K).

For small H_c, we find that the underlying JV stacks represent robust 1D traps for PV stacks over a broad studied temperature range (77–88 K), while the repulsion between pancakes in the same Cu–O plane prevents PV stacks from passing one another along the length of the chain. As a consequence, the dynamic properties of the 1D vortex chain state appear to be particularly rich, as illustrated by the following two complementary experiments where one magnetic field component is held constant and the other varied.

Figure 5a shows images from a movie, illustrating how a trapped chain of PVs can be coherently dragged along by a JV stack as $H_{//}$ is reduced at fixed H_c (= 0.5 Oe) at 83 K. During its movement from the lower left to the upper right corner, the JV stack (J) is able to depin and drag with it two isolated PV stacks (A, B), which were originally pinned at defects on the right-hand side of the image. Pancake vortex displacements can be uniquely and reversibly determined by adjusting the applied field component $H_{//}$: we consider that this vortex 'pump'-like action may find applications in flux-logic devices where a 'bit' is defined by the presence (or absence) of a single PV stack. A simple binary switch could, for example, be realized by using an in-plane field to manipulate a single PV stack underneath a flux transducer (for example, a microscopic induction coil or Hall probe) whose voltage output provides a read-out signal. The small pancake vortex diameters (~400 nm) potentially allow very-large-scale integration of such devices with high operation speeds. In-plane magnetic fields could also be used to indirectly compress PV stacks, yielding an active PV

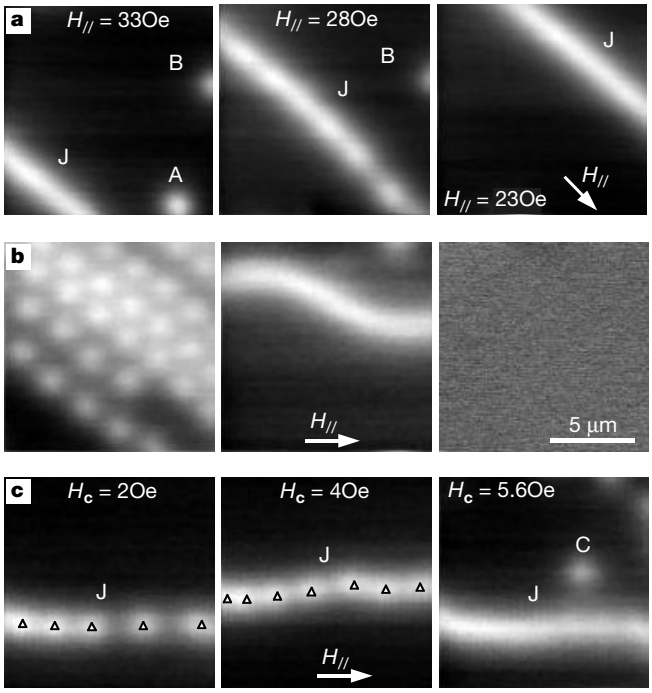

Figure 5 Images from a movie of the motion of pancake vortex stacks as the magnetic field is varied. **a**, The vortex 'pump'-like action achieved by varying $H_{//}$ with fixed H_c (= 0.5 Oe) at 83 K: left, $H_{//} = 33$ Oe (greyscale, 2.9 G); middle, $H_{//} = 28$ Oe (greyscale, 3.2 G); and right, $H_{//} = 23$ Oe (greyscale, 3.4 G). **b**, The demagnetization procedure that uses this vortex 'pump' principle: left, the remnant state after application and removal of $H_c = 4$ Oe at 85 K (greyscale, 4.3 G); middle, application of $H_{//} = 35$ Oe ($H_c = 0$) at 85 K (greyscale, 3.5 G); right, the demagnetized sample after $H_{//}$ is slowly reduced to zero (greyscale, 0.6 G). **c**, Images from a movie of the penetration of PVs along 1D chains as H_c is increased after field-cooling to 81 K at $H_c = 2$ Oe and (fixed) $H_{//} = 35$ Oe: left, $H_c = 2$ Oe (greyscale, 3.2 G); middle, $H_c = 4$ Oe (greyscale, 3.7 G); and right, $H_c = 5.6$ Oe (greyscale, 4.2 G). The PV density along the chain J (indicated by triangles) increases until at saturation the PV stack, C, moves into the domain between JV stacks.

flux amplifier or transducer. Figure 5b illustrates how the pump can be used to demagnetize a sample[15]. The left-hand frame shows the flux trapped in our sample after the application and subsequent removal of $H_c = 4$ Oe at 85 K ($H_{//} = 0$). An in-plane field, $H_{//} = 35$ Oe, was then applied, driving the sample into the vortex chain state (middle frame). Finally, the in-plane field $H_{//}$ was slowly removed and, as the JVs were swept out of the sample they dragged the PVs with them, leaving a demagnetized sample (right-hand frame).

Magnetic irreversibility in layered superconductors is known to be suppressed by the application of either a.c.[6,15] or d.c. in-plane magnetic fields. The movie images shown in Fig. 5c yield insights into the latter situation, where H_c has been increased from 2 Oe at fixed $H_{//} = 35$ Oe at 81 K. We find that PVs preferentially penetrate along the 1D vortex chains (left hand and middle frames), and only propagate into the inter-chain spaces if the chain density becomes saturated (right-hand frame) as explained in Fig. 2 legend. It seems that the PV stack structure induced by the JV currents weakens the interaction with quenched sample disorder, and the mobility of PVs along the 1D chains is considerably higher than in the inter-chain spaces. Magnetization loops measured with the scanning Hall probe retracted from the sample surface confirm this conclusion, and reveal a marked suppression of the irreversibility in the presence of JVs ($H_{//} \neq 0$). PV penetration in this regime is known to be limited by electromagnetic surface barriers[16], which will be slightly lower where JVs intercept the edges, owing to the superposition of Meissner and JV currents. Hence PVs preferentially enter at the sample edges along JVs where surface barriers are lowest, and then show a much higher mobility along the 1D vortex chains. □

Received 2 May; accepted 19 October 2001.

1. Kleiner, W. H., Roth, L. M. & Autler, S. H. Bulk solution of Ginzburg-Landau equations for type II superconductors: upper critical field region. *Phys. Rev. A* **133,** 1226–1227 (1964).
2. Clem, J. R. Anisotropy and two-dimensional behaviour in the high-temperature superconductors. *Supercond. Sci. Technol.* **11,** 909–914 (1998).
3. Bulaevski, L. N., Levdij, M. & Kogan, V. G. Vortices in layered superconductors with Josephson coupling. *Phys. Rev. B* **46,** 366–380 (1992).
4. Huse, D. A. Magnetic-flux patterns on the surface of a type-II superconductor. *Phys. Rev. B* **46,** 8621–8623 (1992).
5. Koshelev, A. E. Crossing lattices, vortex chains, and angular dependence of melting line in layered superconductors. *Phys. Rev. Lett.* **83,** 187–190 (1999).
6. Farrell, D. E. *et al.* Magnetization jumps and irreversibility in $Bi_2Sr_2CaCu_2O_8$. *Phys. Rev. B* **53,** 11807–11816 (1996).
7. Bolle, C. A. *et al.* Observation of a commensurate array of flux chains in tilted flux lattice in Bi-Sr-Ca-Cu-O single crystals. *Phys. Rev. Lett.* **66,** 112–115 (1991).
8. Grigorieva, I. V., Steeds, J. W., Balakrishnan, G. & Paul, D. M. Vortex-chain state in $Bi_2Sr_2CaCu_2O_{8+\delta}$—experimental evidence for coexistence of 2 vortex orientations. *Phys. Rev. B* **51,** 3765–3771 (1995).
9. Oral, A., Bending, S. J. & Henini, M. Real-time scanning Hall probe microscopy. *Appl. Phys. Lett.* **69,** 1324–1326 (1996).
10. Grier, D. G. *et al.* Translational and bond-orientational order in the vortex lattice of the high-T superconductor $Bi_{2.1}Sr_{1.9}CaCu_2O_{8+x}$. *Phys. Rev. Lett.* **66,** 2270–2273 (1991).
11. Martinez, J. C. *et al.* Magnetic anisotropy of a $Bi_2Sr_2CaCu_2O_x$ single crystal. *Phys. Rev. Lett.* **69,** 2276–2279 (1992).
12. Zeldov, E. *et al.* Thermodynamic observation of first-order vortex-lattice melting transition in $Bi_2Sr_2CaCu_2O_8$. *Nature* **375,** 373–376 (1995).
13. Soibel, A. *et al.* Imaging the vortex-lattice melting process in the presence of disorder. *Nature* **406,** 282–287 (2000).
14. Nelson, D. R. Vortex entanglement in high-T_c superconductors. *Phys. Rev. Lett.* **60,** 1973–1976 (1988).
15. Avraham, N. *et al.* Inverse melting of a vortex lattice. *Nature* **411,** 451–454 (2001).
16. Burlachkov, L. *et al.* Giant flux-creep through surface barriers and the irreversibility line in high temperature superconductors. *Phys. Rev. B* **50,** 16770–16773 (1994).

Acknowledgements

We thank M.J.W. Dodgson for discussions. This work was supported in the UK by the EPSRC and the MOD, in the USA by MARTECH, Florida State University, and in Japan by the Ministry of Education, Science, Sports and Culture.

Competing interests statement

The authors declare that they have no competing financial interests.

Correspondence and requests for materials should be addressed to S.B. (e-mail: pyssb@bath.ac.uk).

High-temperature ultrafast polariton parametric amplification in semiconductor microcavities

M. Saba*, C. Ciuti*, J. Bloch†, V. Thierry-Mieg†, R. André‡, Le Si Dang‡, S. Kundermann*, A. Mura§, G. Bongiovanni§, J. L. Staehli* & B. Deveaud*

* *Physics Department, Swiss Federal Institute of Technology Lausanne, PH-Ecublens, CH-1015 Lausanne-EPFL, Switzerland*
† *Centre National de la Recherche Scientifique, L2M-CNRS, 92225 Bagneux Cedex, France*
‡ *Laboratoire de Spectrometrie Physique, Université J. Fourier-Grenoble, F-38402 Saint Martin d'Hères Cedex, France*
§ *Dipartimento di Fisica and Istituto Nazionale di Fisica della Materia, Università degli Studi di Cagliari, I-09042 Monserrato, Italy*

Cavity polaritons, the elementary optical excitations of semiconductor microcavities, may be understood as a superposition of excitons and cavity photons[1]. Owing to their composite nature, these bosonic particles have a distinct optical response, at the same time very fast and highly nonlinear. Very efficient light amplification due to polariton–polariton parametric scattering has recently been reported in semiconductor microcavities at liquid-helium temperatures[2–11]. Here we demonstrate polariton parametric amplification up to 120 K in GaAlAs-based microcavities and up to 220 K in CdTe-based microcavities. We show that the cut-off temperature for the amplification is ultimately determined by the binding energy of the exciton. A 5-μm-thick planar microcavity can amplify a weak light pulse more than 5,000 times. The effective gain coefficient of an equivalent homogeneous medium would be 10^7 cm^{-1}. The subpicosecond duration and high efficiency of the amplification could be exploited for high-repetition all-optical microscopic switches and amplifiers. 10^5 polaritons occupy the same quantum state during the amplification, realizing a dynamical condensate of strongly interacting bosons which can be studied at high temperature.

A semiconductor microcavity is a photonic structure designed to enhance light–matter interaction. The cavity photons are confined between two mirrors, and resonantly interact with the excitonic transition of a two-dimensional semiconductor quantum well (Fig. 1). In the strong-coupling regime, the normal modes of the system are the cavity polaritons, which are half-exciton, half-photon quasiparticles[1]. The energies of the two polariton modes anticross when the energy difference between exciton and photon modes is varied (Fig. 1). The minimum polariton splitting measures the strength of the coupling. Owing to their excitonic content, polaritons are subject to Coulomb interaction and give rise to strong optical nonlinearities. At the same time, owing to the photon component, the curve of polariton energy dispersion versus in-plane wavevector is very steep, meaning that it is quite sensitive to the excitation angle (Fig. 1). A small number of states can be excited at a given angle, and quantum degeneracy (more than one polariton per state) is achieved with relatively low excitation densities. The bosonic statistics strongly enhances some particular scattering processes, provided that the density is kept below the critical value where the bosonic behaviour of excitons breaks down owing to the appearance of the fermionic nature of electrons and holes, which make up the excitons[12]. The scattering from an incoherent exciton reservoir into polaritons can be stimulated by the occupation of the final state[13] and give rise to a polariton laser[14]. If, as in our case, coherent polaritons are injected into the cavity, the phase-coherent final-state stimulation (termed parametric amplification) can be much more efficient than in the incoherent case[2–11].